NATIONAL BUREAU OF STANDARDS REPORT

9911

FRACTOGRAPHY OF A 7178-T6 ALUMINUM FAILED WING PLANK

TO

NATIONAL TRANSPORTATION SAFETY BOARD

BUREAU OF AVIATION SAFETY

U.S. DEPARTMENT OF COMMERCE

NATIONAL BUREAU OF STANDARDS

NATIONAL BUREAU OF STANDARDS REPORT

NBS PROJECT	NBS REPORT
3120412	9911

FRACTOGRAPHY OF A 7178-T6 ALUMINUM FAILED WING PLANK

by

D. B. Ballard

To

National Transportation Safety Board

Bureau of Aviation Safety

U.S. DEPARTMENT OF COMMERCE

NATIONAL BUREAU OF STANDARDS

by

D. B. Ballard

Introduction

Three sections which had been cut from the top surface of a fractured right wing plank adjacent to the forward edge of the access door (in the area of station 119) of Braniff Electra N-9707 were submitted by Mrs. R. Mayner of the National Transportation Safety Board, Bureau of Aviation Safety on 24 June 1968 for fractographic analysis. Two additional pieces of wing plank from the same accident (location unknown) were submitted by Mr. W. L. Holshouser on 22 July 1968 for comparison of fracture surface with the first three specimens.

Observations

Photomacrographs of the first three fracture sections (1-1, 1-2, 1-3) are shown in Figs. 1, 2, and 3. The area examined by Electron Microscopy is indicated by the circle on each figure. Figures 4 and 5 show the additional fractured sections of wing plank and the location of fracture surfaces. Photomacrographs of the replicas of these fractures (#4, #5, #6) and areas examined by Electron Microscopy are shown in Figs. 6, 7, and 8. In all cases except fracture (1-2) a particular effort was made to place the replica on the microscope grid so as to observe the topography

of the outside surface in the vicinity of the fillet, the origin at the edge of fracture, and the fracture surface 0.5 to 1.0 mm away from the edge of fracture.

The fractures were ultrasonically cleaned in acetone to remove loose contamination and oils. At least seven cleaning replicas were stripped from each fracture to obtain a clean metal surface. Three final replicas were made from each area examined. Negative one-step replicas were made using cellulose acetate softened with a mixture of acetone and dibutyl phthalate. After drying the replicas were stripped and rotary shadowed with palladium at 45° and carbon at 90°.

Fractographs of specimen (1-1) are shown in Figs. 9a thru 9f. The original magnification is indicated by the length of the micro meter mark included in each electron photomicrograph. The two photomicrographs 9a and 9b were taken adjacent to the fillet on the fracture surface. The general surface topography is typical of intergranular fracture which usually indicates stress corrosion cracking. Superimposed on the grain facets can be seen a fine dimple-like surface indicating low ductility fracture. There is a small increase in surface roughness in Fig. 9c which was adjacent to Figs. 9a and b but more distant from fillet edge. The first evidence of transgranular ductile fracture is shown in Fig. 9d as narrow bands of dimpled rupture parallel to the long axis of the fracture between areas of low ductility. These features are shown again in Figs. 9e and 9f and are typical of the fracture surface approximately 0.5 mm away from the edge of fracture.

Visual examination of the section (1-2) showed that the fracture edge adjacent to the fillet was mechanically abraded and all original fracture surface was destroyed. Therefore an undamaged area was chosen at a location approximately half the distance across the fracture. Figures 10a through 10f show microstructure typical of this area. In general the surface shows an elongated transgranular fractured grains of low ductility bounded by narrow bands of dimpled rupture. The amount of dimpled rupture shows a significant increase of ductility over the fracture edge of (1-1).

The surface of fracture section (1-3) was coated in places by a dark brown debris. This was removed by successive cleaning replicas until a clean metal surface in the area of interest was obtained. The outside exposed surface in the area of the fillet is shown in Figs. 11a and b. Identification of the lamellar structure is unknown. (It may be the partially corroded anodized coating). The fillet edge of the fracture is shown in Figs. 11c, d, e. Severe corrosion or oxidization has changed the surface and altered the original fracture surface features. A smaller amount of surface corrosion appears to have occurred on the areas shown in Figs. 11g and 11h. This surface area was approximately 1 mm distant from the fillet edge and appears to retain some of the original fracture topography. At a distance of 1.5 mm the surface appears as in Figs. 11k and 11ℓ. Little or no corrosion is noted and the small amount of dimpled rupture is evident.

Fracture #4 was, by visual examination, similar to (1-3); that is, a flat semi lustre surface. The outside surface at the fillet is shown

in the upper left corner of Fig. 12a. The edge of fracture begins at the diagonal, progresses to lower right, and exhibits a flat surface with fine traces of corrosion. The large irregular shapes in Fig. 12b may be a thick oxide or surfaces which have been deeply corroded. A fine dimpled structure can be seen on all Figs. (a) through (f) indicating a low ductility fracture. An indication of intergranular fracture is shown in Fig. 12e. The mud crack pattern in Fig. 12f is probably the result of rapid corrosion of an exposed large second phase particle or an inclusion.

Macroexamination of fracture #5 revealed the presence of a small flat brittle region between the fillet and the fibrous woody fracture surface. Fractographs of this flat area and part of the outside surface are shown in Figs. 13a through 13e. Two small areas of corrosion are noted at arrows, these are adjacent to smooth areas which extend to the outside surface. This may indicate the presence of a pre-existing stress corrosion crack before overload. A steep sloping step is also noted by a dark band that extends through the center of the photographs and connects the fillet edge with the flat fracture. This may indicate the fracture initiated by shear failure in these areas. Fig. 13f is typical of the fracture surface away from the edge. The fracture is transgranular with a small amount of dimpled rupture and few small areas of initial corrosion.

Fracture #6 had occurred in the wing plank material on a plane parallel to and nearly at same horizontal plane as the outside surface. By visual examination it also resembled fracture section (1-3) in

appearance. The upper left corner of Fig. 14a is the outside surface. The wedge shape edge entering from upper right is intercrystalline fracture with a small amount of dimple rupture, then changes in the lower part of the photo to transcrystalline with a larger amount of dimple rupture.

Figure 14b is an example of cleavage at the fracture edge as compared with low ductility shear in Fig. 14c. Cleavage and evidence of corrosion can be seen in Figs. 14d and 14e. Evidence of mud cracks can be noted in both Figs. 14e and f. In Fig. 14f the prior fracture surface details have been covered or removed by corrosion or oxidization.

Conclusions

1. Dimpled rupture, as an indication of ductility, was found at the fillet edge of all fractures except fracture section (1-3). This section had evidence of severe corrosion at the fillet edge of fracture.

2. There is a possibility that a stress corrosion crack approximately 1.5 mm deep and of unknown length may have existed in section (1-3) prior to final overload failure.

3. The occurrence of surface corrosion and/or mud cracks does not constitute the positive identification of stress corrosion cracking in a fracture surface of 7178-T6 aluminum alloy extrusion. The corrosion may have occurred on the fracture surface after failure as evidenced by examination of two additional fractured samples of wing plank.

4. The precise location of replicas as related to the macro features of a fracture is essential to the interpretation of the electron fractographs as fracture mode and topography can change radically with location of electron microscope examination.

Fig. 1. Fracture Section (1-1)
Encircled area replicated for
electron fractography. X2

Fig. 2. Fracture Section (1-2)
X4

Fig. 3. Fracture Section (1-3)
X4

Fig. 4. Location of fracture
areas #4 and #5. X1/5

Fig. 5. Fracture location #6
X1/5

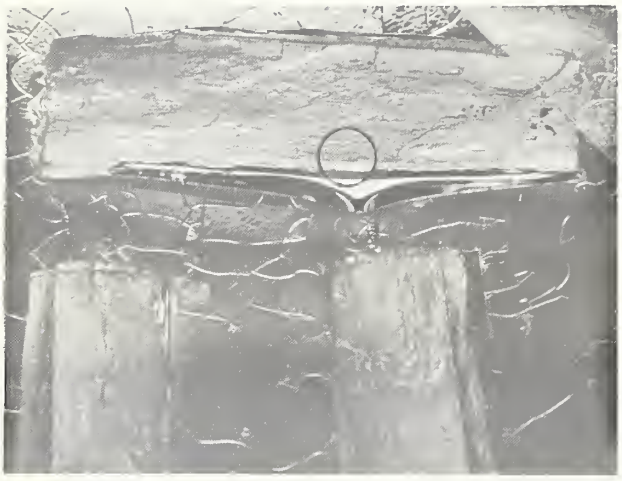

Fig. 6. Replica of fracture surface #4
X4

Fig. 7. Replica of fracture surface #5. The outside surface is in the lower sector of circle. X4

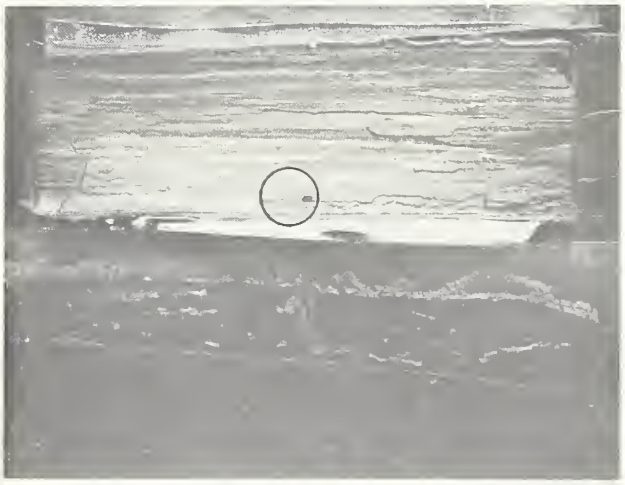

Fig. 8. Replica of fracture surface #6
X4

Fracture Section (1-1)

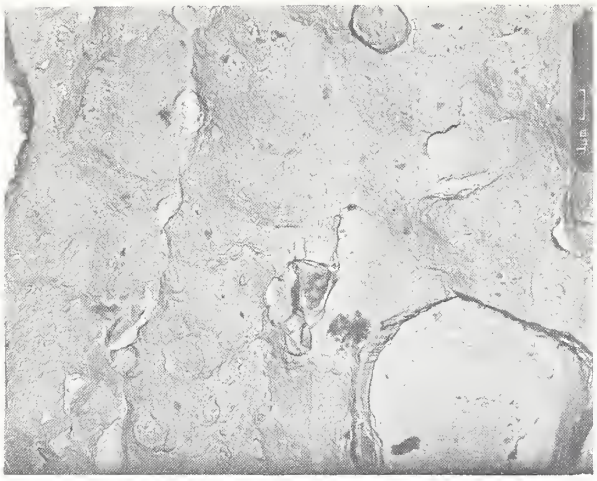

Fig. 9a. Adjacent to fillet

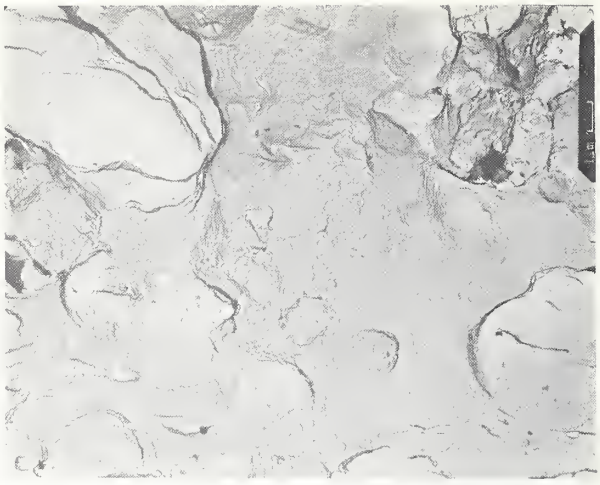

Fig. 9b.

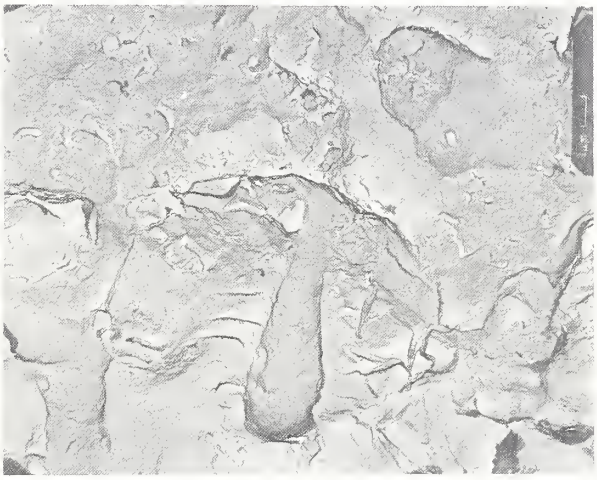

Fig. 9c.

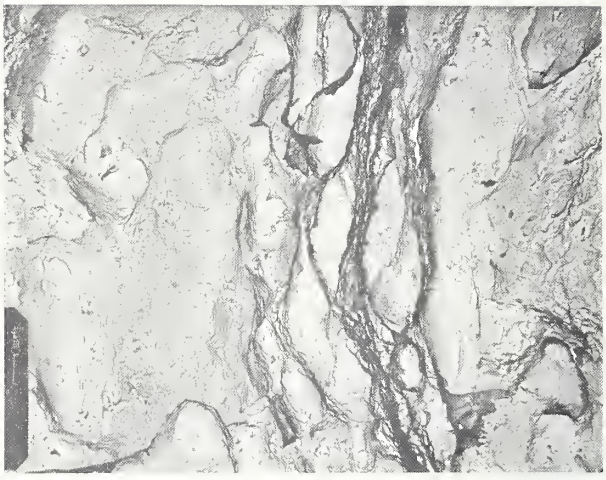

Fig. 9d.

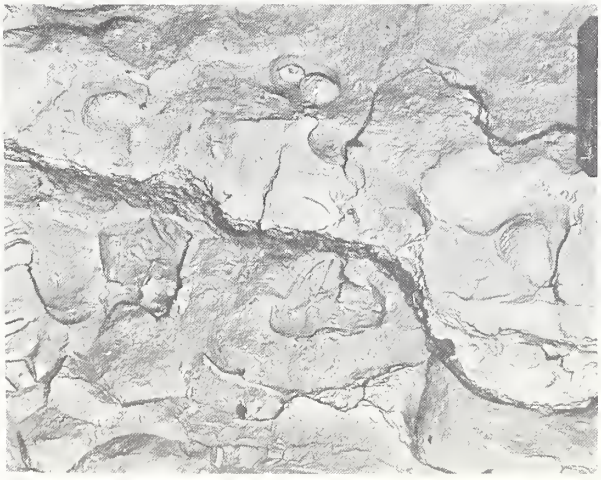

Fig. 9e.

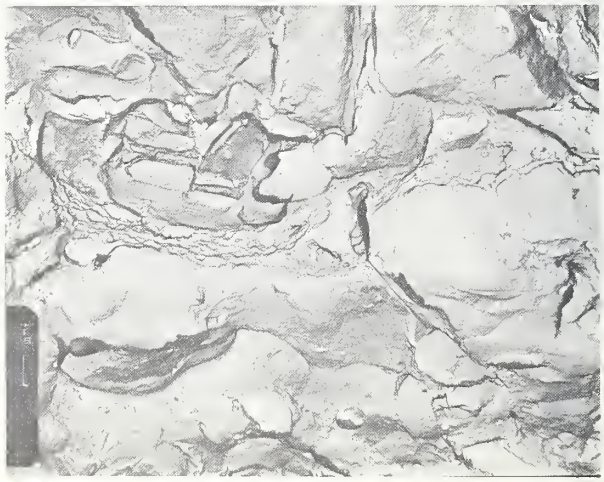

Fig. 9f. Approximately 0.5 mm distant from fillet.

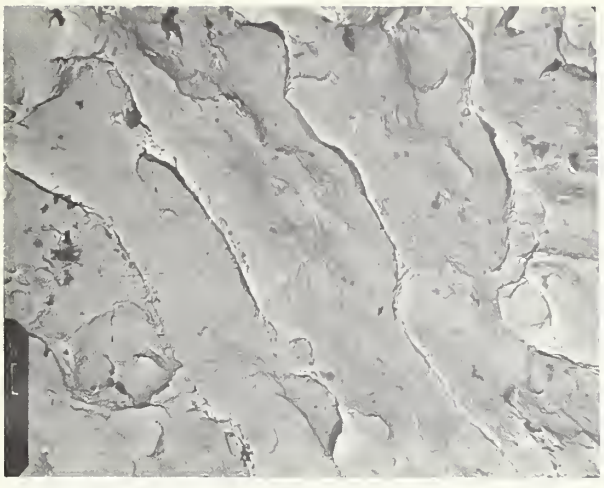

Fig. 10a.

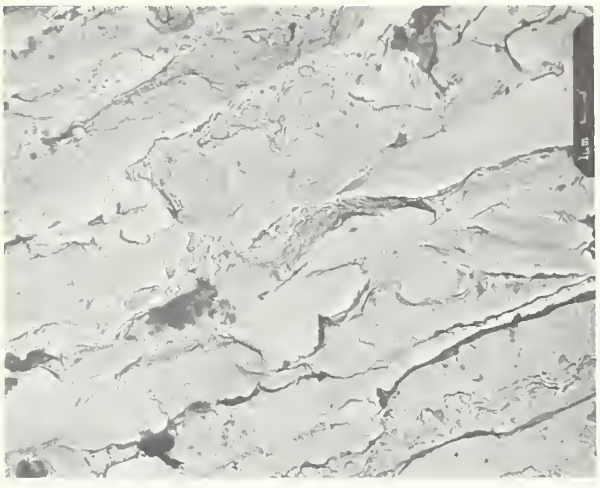

Fig. 10b.

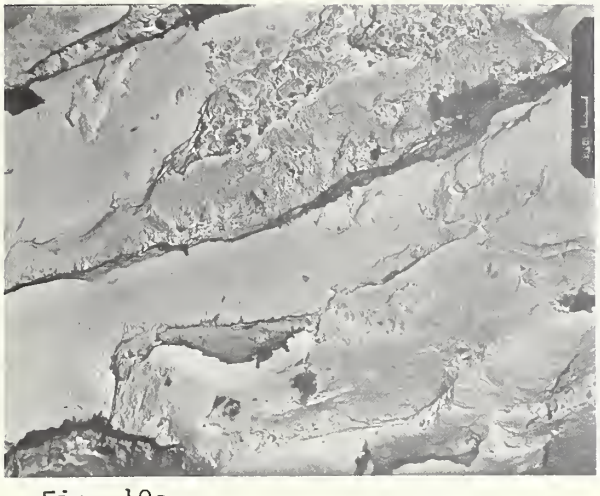

Fig. 10c.

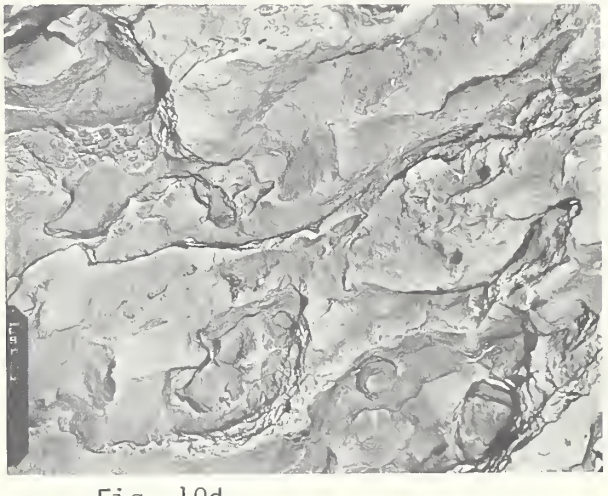

Fig. 10d.

Fig. 10e.

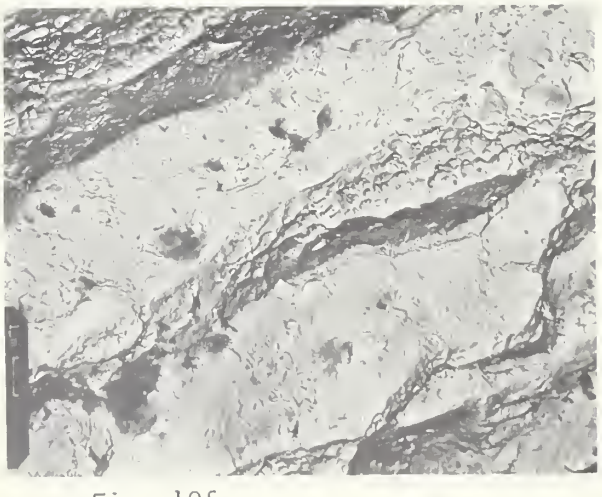

Fig. 10f.

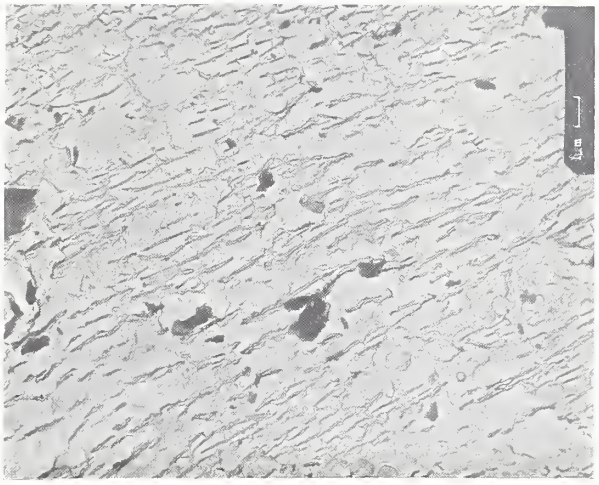

Fig. 11a. Outside surface

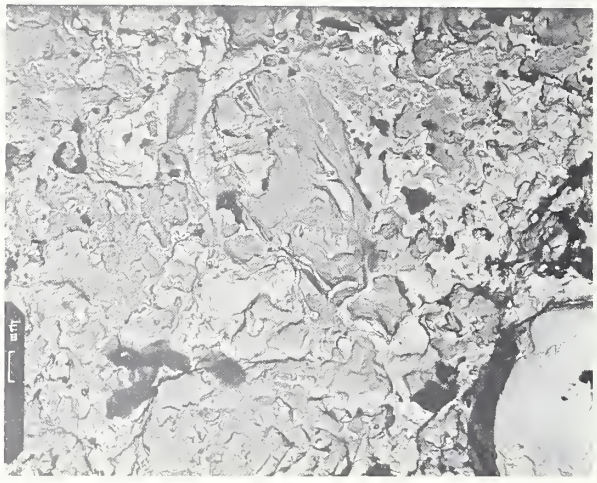

Fig 11b. Outside surface

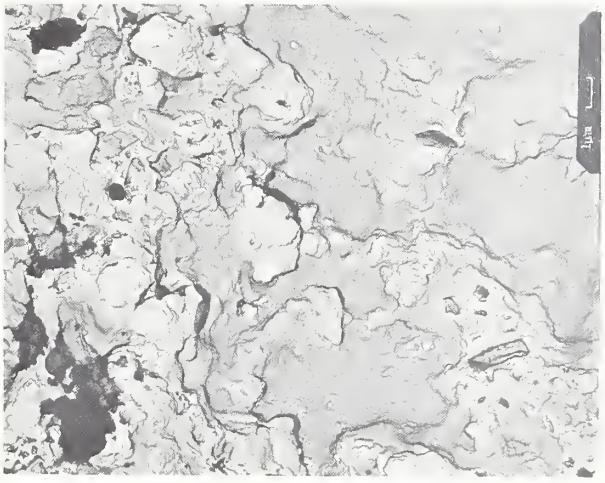

Fig. 11c.

Edge of fracture

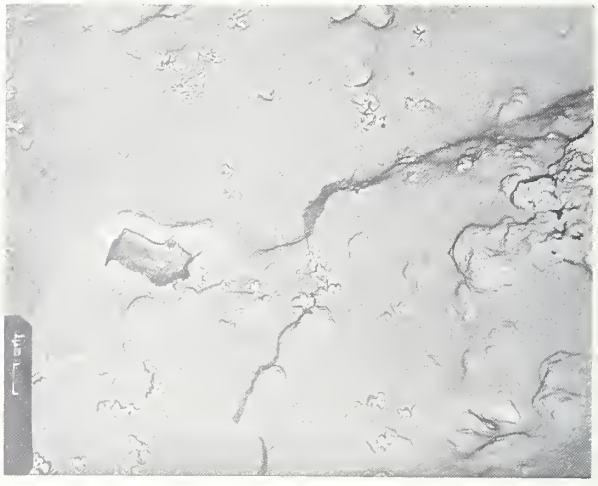

Fig. 11d.

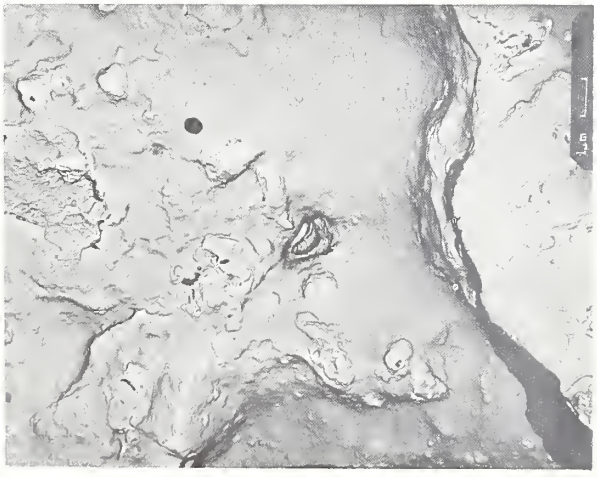

Fig. 11e.

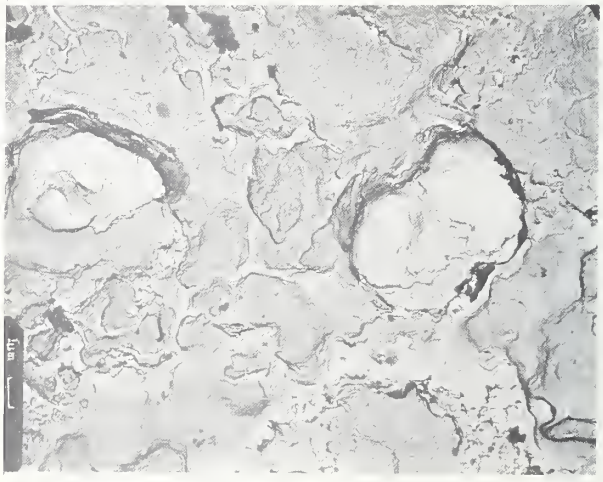

Fig. 11f.

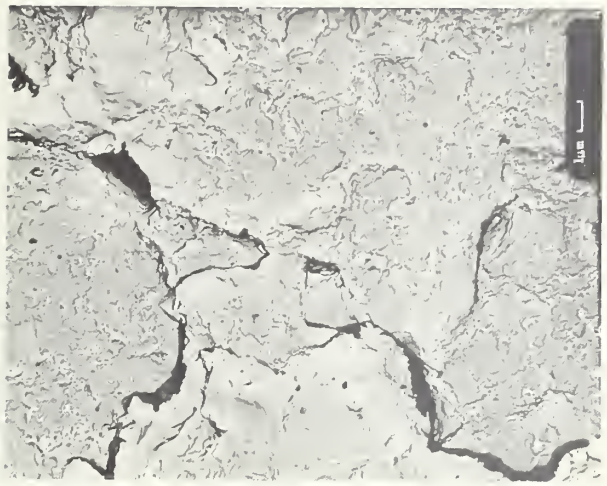

Fig. 11g. Fracture surface approximately 1.0 mm distant from fillet.

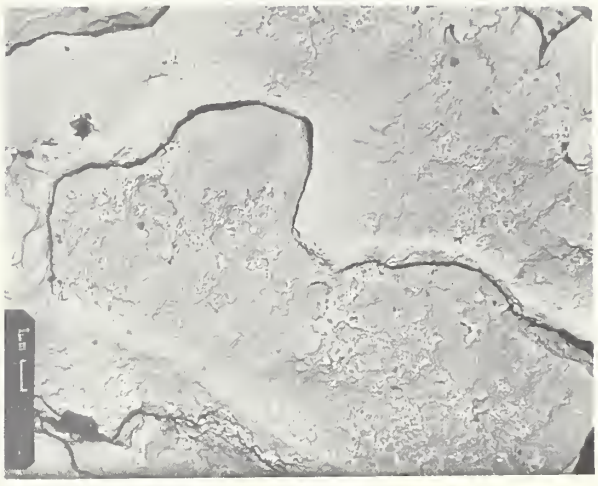

Fig. 11h.

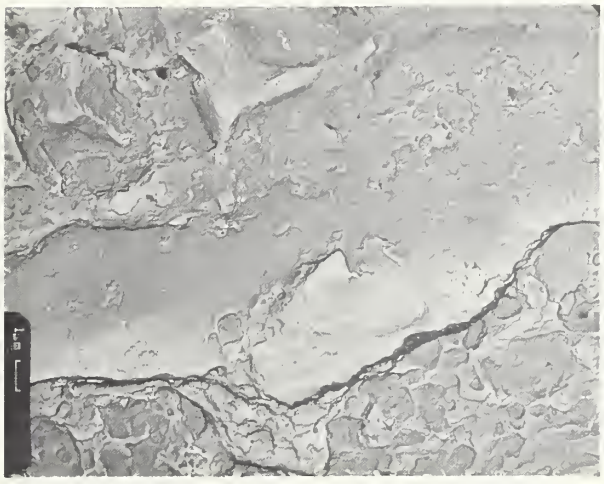

Fig. 11i.

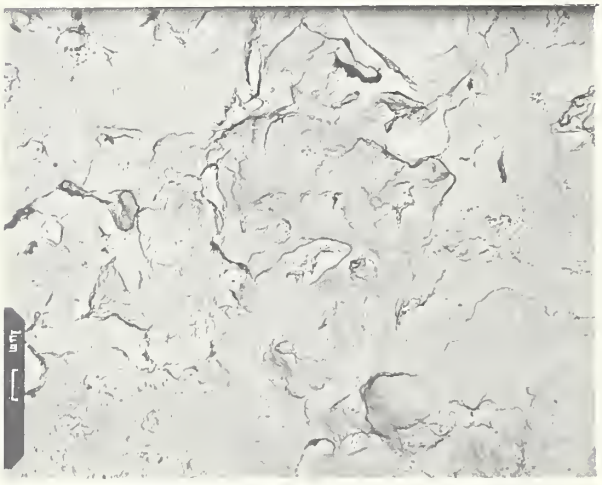

Fig. 11j

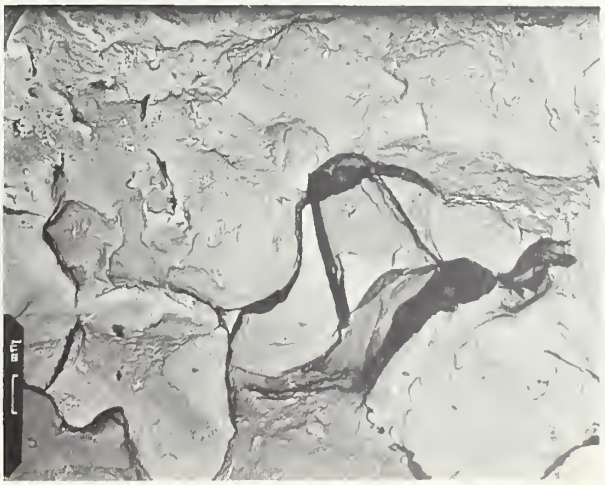

Fig. 11k.

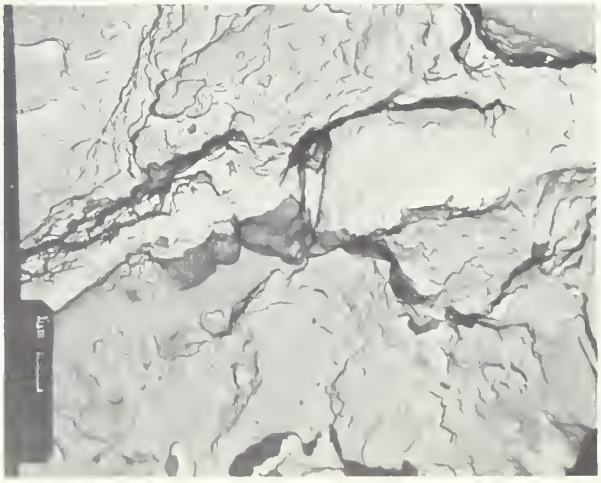

Fig. 11ℓ. Fracture surface approximately 1.5 mm from fillet edge.

Fracture Surface #4

Fig. 12a. Fracture surface

Fig. 12b.

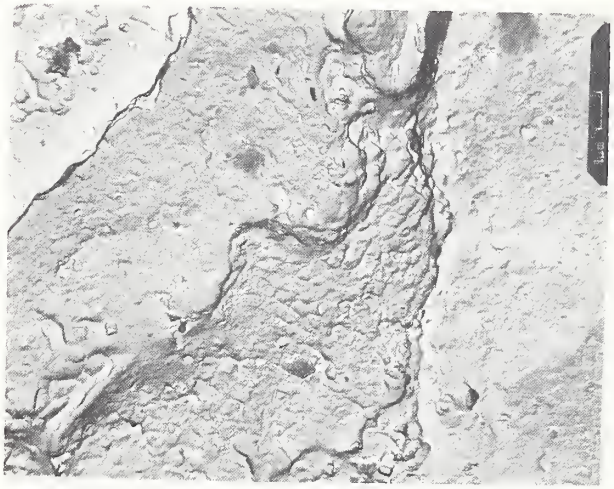

Fig. 12c.

Fig. 12d.

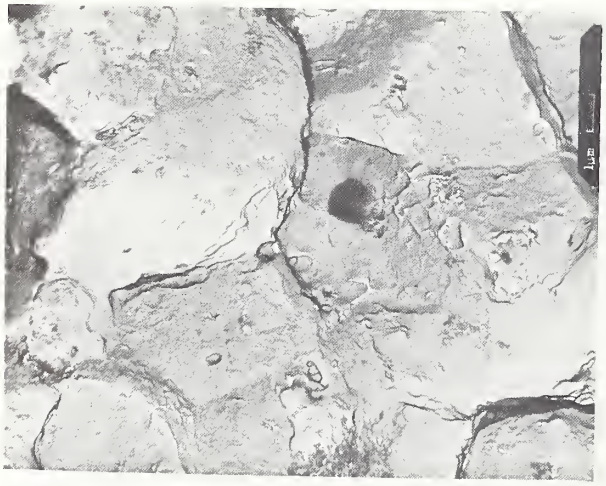

Fig. 12e.

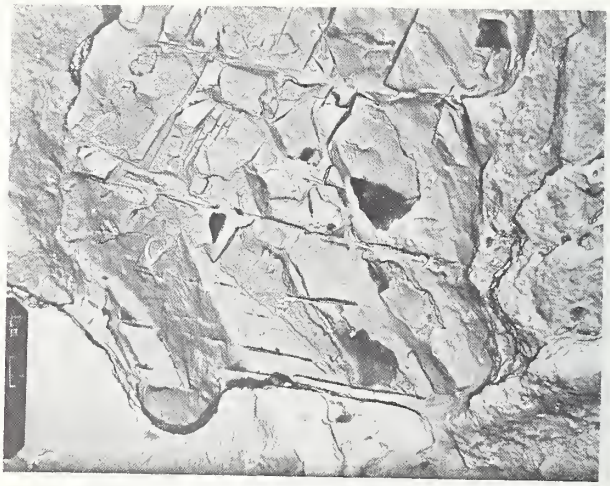

Fig. 12f. Corrosion on second phase, or inclusion.

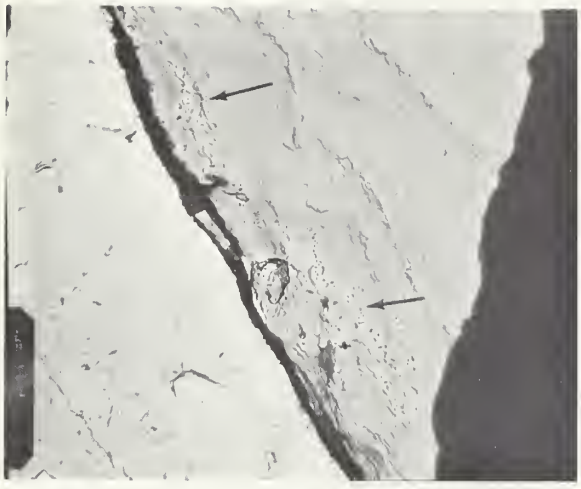

Fig. 13a. Outside surface

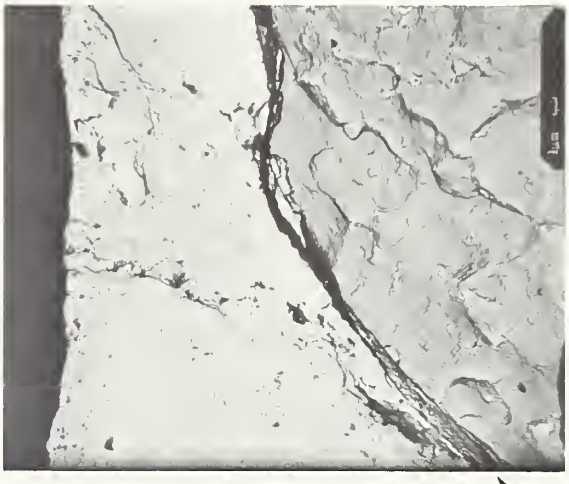

Fig. 13b.

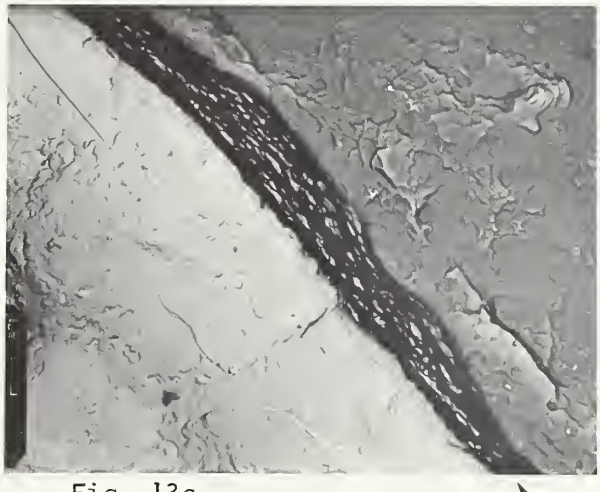

Fig. 13c

Fig. 13d.

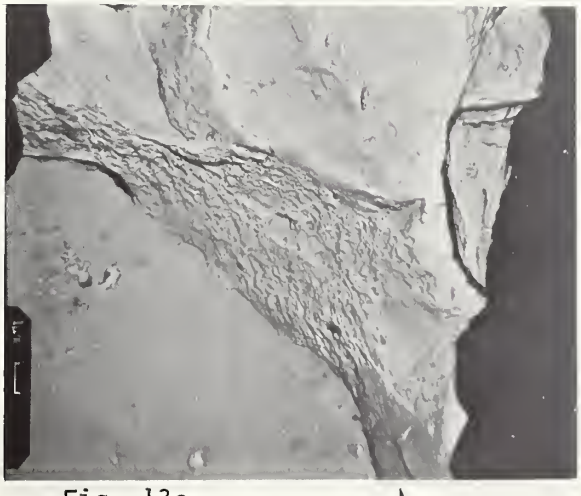

Fig. 13e.

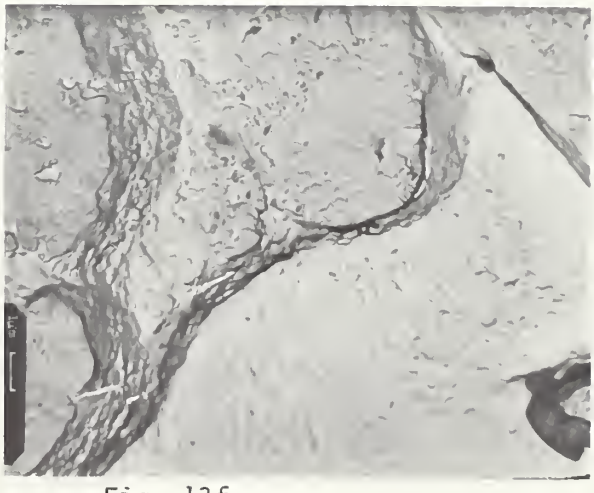

Fig. 13f.

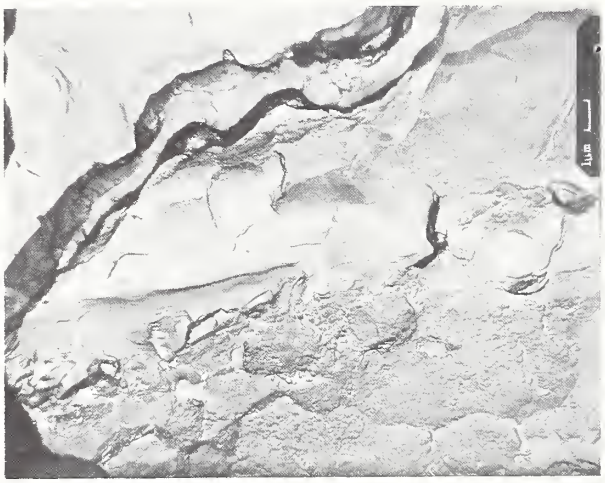

Fig. 14a.

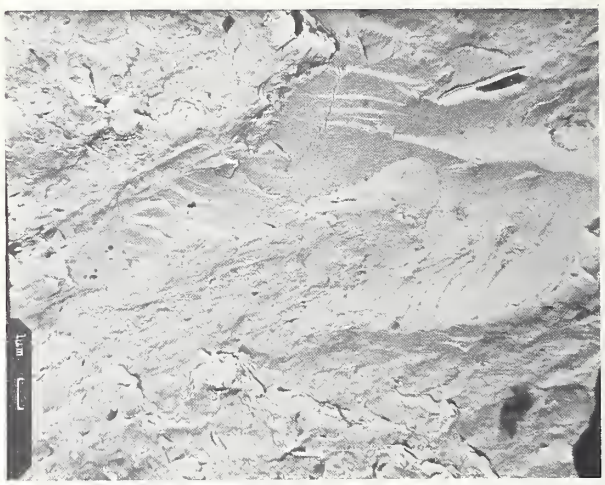

Fig. 14b.

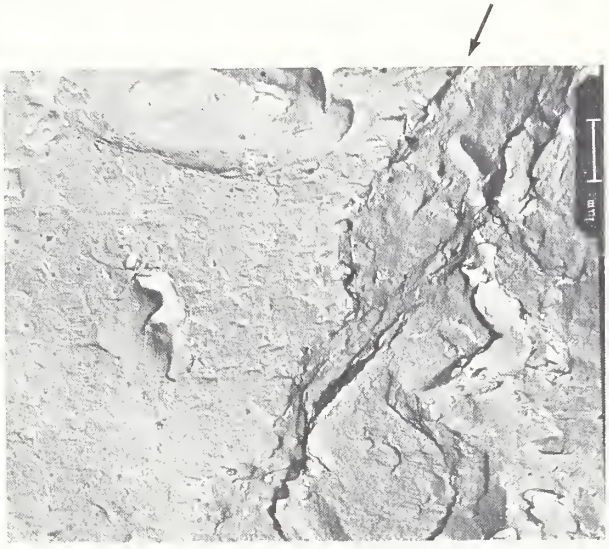

Fig. 14c.

Outside surface

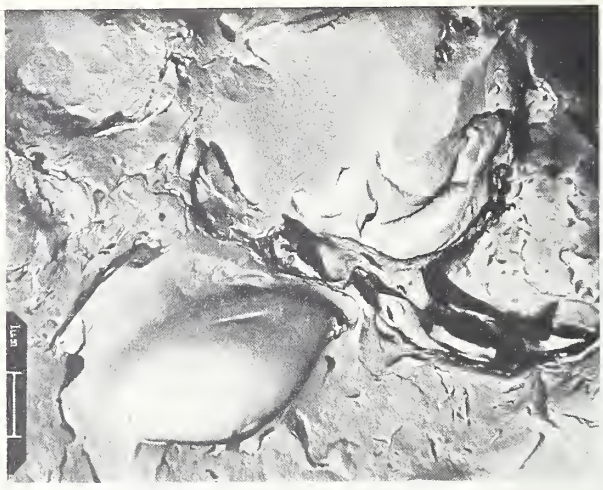

Fig. 14d.

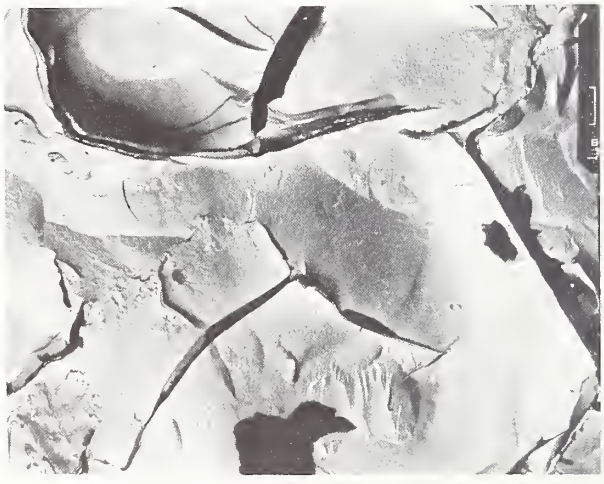

Fig. 14e.

Fig. 14f.